Title

Scaled ZrO2 dielectrics for In0.53Ga0.47As gate stacks with low interface trap densities

Permalink

https://escholarship.org/uc/item/98g5w28d

Journal

Applied Physics Letters, 104(18)

ISSN

0003-6951 1077-3118

Authors

Chobpattana, Varistha
Mates, Thomas E
Zhang, Jack Y
et al.

Publication Date

2014-05-05

DOI

10.1063/1.4875977

Peer reviewed

AIP | Applied Physics Letters

Scaled ZrO2 dielectrics for In0.53Ga0.47As gate stacks with low interface trap densities

Varistha Chobpattana, Thomas E. Mates, Jack Y. Zhang, and Susanne Stemmer

Citation: Applied Physics Letters **104**, 182912 (2014); doi: 10.1063/1.4875977
View online: http://dx.doi.org/10.1063/1.4875977
View Table of Contents: http://scitation.aip.org/content/aip/journal/apl/104/18?ver=pdfcov
Published by the AIP Publishing

APPLIED PHYSICS LETTERS **104**, 182912 (2014)

Scaled ZrO_2 dielectrics for $In_{0.53}Ga_{0.47}As$ gate stacks with low interface trap densities

Varistha Chobpattana, Thomas E. Mates, Jack Y. Zhang, and Susanne Stemmer
Materials Department, University of California, Santa Barbara, California 93106-5050, USA

(Received 8 March 2014; accepted 29 April 2014; published online 9 May 2014)

ZrO_2 dielectrics were grown on n-$In_{0.53}Ga_{0.47}As$ channels by atomic layer deposition, after employing an *in-situ* cyclic nitrogen plasma/trimethylaluminum surface cleaning procedure. By scaling the ZrO_2 thickness, accumulation capacitance densities of 3.5 μF/cm^2 at 1 MHz are achieved. The midgap interface trap density is estimated to be in the 10^{12} cm^{-2} eV^{-1} range. Using x-ray photoelectron spectroscopy, it was shown that the interface contained the oxides of In, Ga, and Al, but no As-oxides or As-As bonds within the detection limit. The results allow for insights into the effective passivation of these interfaces. *© 2014 AIP Publishing LLC*.
[http://dx.doi.org/10.1063/1.4875977]

III–V metal-oxide-semiconductor field effect transistors (MOSFETs) are currently being investigated for post-Si complementary metal-oxide-semiconductor technology.[1] III–V MOSFETs require high-permittivity (κ) gate dielectrics that allow for low leakage currents and low interface trap densities (D_{it}). Al_2O_3 gate dielectrics, while allowing for unpinned interfaces,[2] severely limit equivalent oxide thickness (EOT) scaling due to the low dielectric constant ($\kappa \sim 9$) of Al_2O_3. We have recently reported on *in-situ*, plasma-based surface treatments[3] prior to atomic layer deposition (ALD) of HfO_2 gate dielectrics on $In_{0.53}Ga_{0.47}As$.[4,5] This process allowed for low D_{it} and scaling of the accumulation capacitance densities to $\sim$3 μF/cm^2 (EOT of less than 1 nm) on n-type doped $In_{0.53}Ga_{0.47}As$ channels, as well as high-performance MOSFETs.[6] We note that the accumulation capacitance density of metal-oxide capacitors (MOSCAPs) on n-$In_{0.53}Ga_{0.47}As$ is not equivalent to the oxide capacitance, due to the low conduction band density of states of the $In_{0.53}Ga_{0.47}As$. These results suggest that this process may enable further scaling of the EOT, using dielectrics with higher κ than HfO_2, while maintaining a low D_{it}.

ZrO_2 has a wide band gap and a higher dielectric constant than HfO_2.[7,8] The use of ZrO_2 as a dielectric in III–V MOSCAPs has been investigated previously, but MOSCAPs typically show a very high D_{it}.[9–12] Large D_{it} is relatively easy to detect for n-type $In_{0.53}Ga_{0.47}As$ channels as a pronounced frequency dispersion at negative gate biases and the failure of the gate stack to reach deep depletion.[13,14] In contrast, high-quality stacks show only a small "D_{it} hump," and they exhibit deep depletion as the Fermi level moves into the lower half of the band gap in capacitance-voltage measurements.[5,13] In this work, we show that a cyclic, *in-situ* nitrogen plasma/trimethylaluminum (TMA) pre-cleaning procedure allows for ZrO_2 dielectrics on n-$In_{0.53}Ga_{0.47}As$ with low D_{it} *and* low EOT. We characterize the interface chemistry, which, in conjunction with the electrical results, allows for insights into the passivation of such interfaces.

Substrates consisted of 300-nm-thick, n-type $In_{0.53}Ga_{0.47}As$ (Si: 1×10^{17} cm^{-3}) layers grown by molecular beam epitaxy on (001) n$^+$-InP (IntelliEpi, Richardson, Texas). Samples were cleaned in buffered HF for 3 min before they were transferred to the ALD reactor (Oxford Instruments FlexAL ALD). The substrate temperature was 300 °C. Alternating *in-situ* nitrogen plasma/TMA-pulse cycles were used immediately prior to ALD, as described in detail elsewhere.[5] The chamber reactor was held at 80 mTorr during ALD. The 40-cycle deposition consisted of the following steps: A TEMAZr (tetrakis[ethylmethylamino]zirconium) pulse, followed by an Ar gas purge, a pump step, and a short pulse of deionized water, followed by additional purge and pump steps. The oxide thicknesses were determined using variable angle spectroscopic ellipsometry. After ALD, 500 nm of SiO_2 was deposited on the sample backside by plasma-enhanced chemical vapor deposition to protect the InP substrate. The samples were annealed in a tube furnace at 400 °C for 15 min in flowing forming gas (95% of N_2 and 5% of H_2). MOSCAPs were fabricated by thermal evaporation of 80 nm thick Ni top contacts (7.8×10^{-5} cm^2) through a shadow mask. The back Ohmic contact, consisting of Cr (20 nm)/Au (100 nm), was deposited using thermal evaporation after SiO_2 removal. An impedance analyzer (Agilent 4294 A) was used for frequency-dependent capacitance-voltage (CV) and conductance-voltage measurements in the dark from 1 kHz to 1 MHz. High-angle annular dark-field scanning transmission electron microscopy (HAADF-STEM) was carried out using a 300 kV field-emission transmission electron microscope. X-ray photoelectron spectroscopy (XPS) was used to investigate the interface. Scans were run using monochromatic Al Kα radiation at a pass energy of 20 eV (Ga 3p was run at 40 eV). The energy scales were calibrated by setting the surface aliphatic hydrocarbon peak to 285.0 eV.

Figure 1 shows the electrical characteristics of MOSCAPs with $\sim$4-nm-thick-ZrO_2. As seen from the CV data in Fig. 1(a), the accumulation capacitance density is 3.5 μF/cm^2 at 1 MHz, which is larger than that of any other III–V gate stack reported in the literature.[5,15,16] A small CV hysteresis of 0.2 V at 1 MHz could be detected (see inset). At low frequencies, the measured accumulation capacitance, C_m, suffers from artifacts from gate leakage, which is expected, given the low physical thickness. The grey markers in Fig. 1(a) indicate where $C_m < G/\omega$, where G_m is the measured conductance, and ω is the frequency. C_m values above those points are not a reliable measure of the capacitance because of the large error in the measurements of the capacitance. We note, however, that the leakage current density was less than

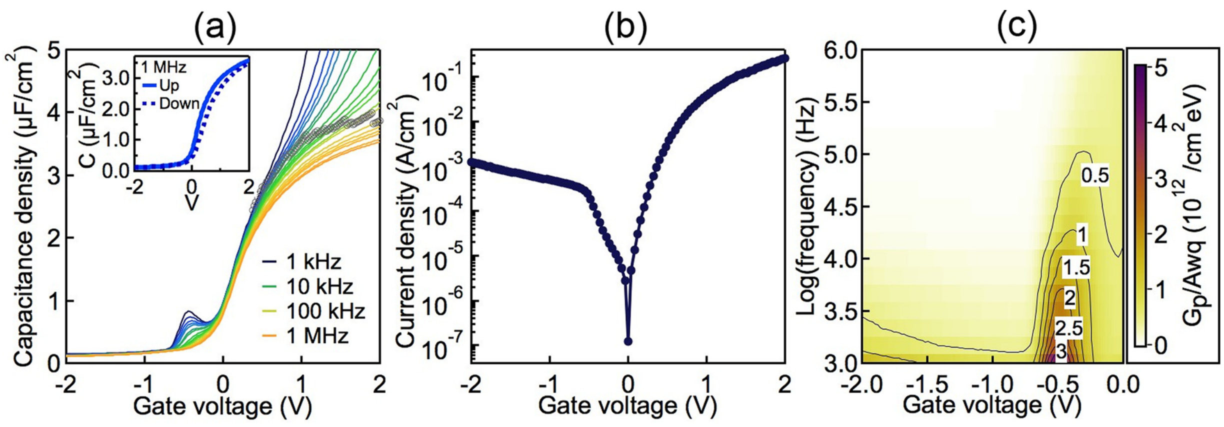

FIG. 1. Electrical characteristics of $In_{0.53}Ga_{0.47}As$ MOSCAPs with ~4 nm ZrO_2. (a) CV characteristics as a function of frequency. Grey symbols indicate where $G/A\omega$ value becomes higher than the capacitance density. The inset shows CV hysteresis at 1 MHz. (b) Current-voltage characteristics between −2 V and 2 V. (c) Normalized parallel conductance maps, showing $\left(G_p/A\omega q\right)_{max}$ as a function of gate voltage and frequency.

0.04 A/cm^2 at 1 V [Fig. 1(b)], orders of magnitude below Si roadmap specifications. Thus leakage is unlikely to be an issue for MOSFETs, which have a much smaller area than these MOSCAPs.

In addition to their high capacitance density, the CV exhibit characteristics consistent with low D_{it}, including a steep slope and a small midgap D_{it} hump at negative biases.[14,17,18] Deep depletion is reached, as can be seen from the finite slope at negative biases. The large band bending is, of course, facilitated by the high oxide capacitance density. These qualitative observations can be confirmed using conductance maps [Fig. 1(c)], which show the normalized conductance peaks, $\left(G_p/A\omega q\right)_{max}$, where G_p is the parallel conductance, A the capacitor area, and q the elemental charge, as a function of gate voltage and ω. Such maps provide a measure of Fermi level efficiency.[19] Here, $\left(G_p/A\omega q\right)_{max}$ shifts more than two orders of magnitude in frequency as the gate bias is changed between −0.25 and −0.75 V, consistent with a large band bending in response to a change in gate bias. The $\left(G_p/A\omega q\right)_{max}$ values (see scale bar on the right) can be used to estimate the D_{it} by multiplication with a factor of ~2.5.[20] The D_{it} values are in the $10^{12}\,cm^{-2}eV^{-1}$ range around midgap. We note that there are great inconsistencies in the reported D_{it} in the dielectric/III–V literature. In particular, very low values have been reported even in cases where the CV shows a large D_{it} response. One issue is an overestimation of the oxide capacitance, which makes $\left(G_p/A\omega q\right)_{max}$ appear too low.[14] To avoid this pitfall, we have previously used a thickness series to determine the interfacial layer capacitance density and the dielectric constant of ALD HfO_2 dielectrics.[5] Assuming that the semiconductor and interfacial layer capacitances are the same here (the interfacial layer is a result of the cleaning procedure, as discussed below), the increase in capacitance at 1 MHz for films of the same physical thickness corresponds to an increase of κ from 18 (ALD HfO_2) to 23 for the ZrO_2 in this study, which is a reasonable value for amorphous or nanocrystalline films.[21]

We note that because of the extremely scaled capacitance density of these gate stacks, CV-based D_{it} extraction methods are unreliable for determining the D_{it} of n-doped channels, at least in their current implementation.[22] One reason is that D_{it} near the conduction band influences the measured capacitance even at 1 MHz due to short trap time constants.[23] As a result, a true high-frequency curve is not obtained, which precludes methods such as the high-low or Terman methods for n-type channels. It has been suggested previously that the D_{it} in the conduction band is high.[24] The results shown here, in particular the fact that the capacitance

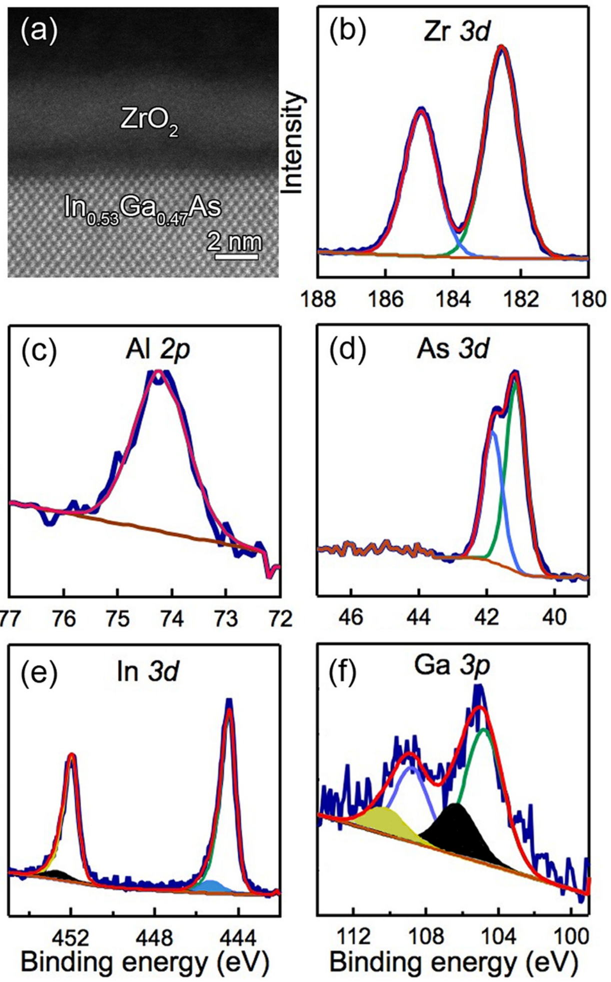

FIG. 2. (a) HAADF/STEM cross-section image of the $ZrO_2/In_{0.53}Ga_{0.47}As$ interface after a forming gas anneal at 400 °C. (b)–(f) XPS of $In_{0.53}Ga_{0.47}As$ MOSCAPs with ~4 nm ZrO_2. (b) Zr 3*d* peaks; (c) Al 2*p* peak; (d) As 3*d* peaks; (e) In 3*d* peaks; and (f) Ga 3*p* peaks. The thin lines are fits to the data.

density scales with κ of the dielectric, show that the Fermi level is not pinned in the conduction band for these gate stacks. With regards to obtaining midgap-D_{it} from CV, deep depletion precludes matching to calculations that do not take deep depletion into account.

Figure 2(a) shows a HAADF/STEM cross-section image of the $ZrO_2/In_{0.53}Ga_{0.47}As$ interface. The ZrO_2 film appears amorphous and uniform. A low-atomic number (dark contrast) interfacial layer forms during the nitrogen plasma/TMA clean. Previous investigations of $HfO_2/In_{0.53}Ga_{0.47}As$ interfaces cleaned with the same method showed that the interface contained O, Al, and small amounts of N.[5] Because of peak overlap with Hf peaks in XPS, these prior studies could not determine if Ga or In oxides were present. To clarify this, we show in Figs. 2(b)–2(f) XPS spectra of the Zr 3*d*, Al 2*p*, As 3*d*, In 3*d*, and Ga 3*p* peaks. The fit of the Zr 3*d* peak [Fig. 2(b)], with Zr $3d^{5/2}$ at 182.6 eV, is consistent with ZrO_2. Figure 2(c) shows that a fit of the Al 2*p* peak at 74.2 eV indicates that Al is fully oxidized. The As 3*d* region [Fig. 2(d)] could be fit using two peaks at 41.1 eV and 41.8 eV, respectively, both with a full width at half maximum (FWHM) of 0.7 eV, arising from the $In_{0.53}Ga_{0.47}As$.[25] No signatures could be detected that could be associated with As_2O_5, As_2O_3, As suboxide, or As-As bonding,[26] similar to what was found previously for $HfO_2/In_{0.53}Ga_{0.47}As$ interfaces.[5] In contrast, In 3*d* peaks [Fig. 2(e)] could be fitted using two components. An In $3d^{5/2}$ peak component appears at 444.4 eV, with a FWHM of ~0.7 eV, consistent with InGaAs.[27] A higher binding energy component [shaded in Fig. 2(e)], for which the In $3d^{5/2}$ falls at 445.3 eV (FWHM of 1.2 eV), indicates bonding with oxygen in form of In_2O_3.[28] Quantification of the survey scan and the high-resolution peak of In 3*d* suggest that the amount of In_2O_3 is at approximately 0.2 at. % (12% of In is oxidized). The Ga 3*p* region [Fig. 2(f)] could also be fitted with two components, with Ga $3p^{3/2}$ peaks at 104.8 eV and 106.3 eV, consistent with Ga-As and Ga_2O_3 bonding, respectively. The amount of Ga_2O_3 is approximately 0.5 at. % (27% of Ga is oxidized). Because of N 1*s*-Ga Auger interference, the presence of N cannot be confirmed by XPS, but it was detected previously in secondary ion mass spectrometry.[5] Although the relative amounts of In, Ga, and Al oxides cannot be quantified, additional insight can be obtained from the contrast in HAADF-STEM. In particular, these images show increased brightness in the interface layer near the interface with $In_{0.53}Ga_{0.47}As$, which indicates the presence of In. Thus, we conclude that the bulk of the interface layer is mostly Al-oxide while the Ga and In oxide XPS signals are from a near-interface region. Investigations of the interface layer thickness as a function of the number of cleaning cycles (not shown here) show that the interface layer forms during the cleaning process (its thickness increases with the number of cycles). Thus, there is sufficient oxygen present in this process to oxidize the TMA and the semiconductor surface.

In summary, we have shown a pre-deposition *in-situ* clean using alternating cycles of remote nitrogen plasma and TMA allows for ALD of highly scaled dielectrics with higher dielectric constants, such as ZrO_2, low D_{it} in $10^{12}\,cm^{-2}\,eV^{-1}$, and sub-nm-EOT. Experiments in the literature have shown a correlation between Ga-O bonds and midgap D_{it}.[18] The relatively small concentration of Ga-O bonding found in the present study may be responsible for the small residual midgap D_{it}. The interfacial layer provides effective passivation, by preventing the formation of detrimental As-oxides and As-As bonding, which theoretical calculations have shown to cause high D_{it},[29–31] during subsequent ALD. We suggest that the procedure should be suitable for other dielectrics that have even higher dielectric constants than ZrO_2, with no or minimal increase in D_{it}.

S.S. and V.C. acknowledge Matthias Passlack, William Mitchell, and Roman Engel-Herbert for helpful discussions. The authors gratefully acknowledge support for this work by the Semiconductor Research Corporation through the Nonclassical CMOS Research Center (Task ID 1437.008). A portion of this work was performed in UCSB's Nanofabrication Facility, which is part of the NSF-funded NNIN network. The work also made use of the MRL Shared Experimental Facilities, which are supported by the MRSEC Program of the NSF under Award No. DMR 1121053.

[1] M. Heyns and W. Tsai, MRS Bull. **34**, 485 (2009).
[2] E. J. Kim, E. Chagarov, J. Cagnon, Y. Yuan, A. C. Kummel, P. M. Asbeck, S. Stemmer, K. C. Saraswat, and P. C. McIntyre, J. Appl. Phys. **106**, 124508 (2009).
[3] A. D. Carter, W. J. Mitchell, B. J. Thibeault, J. J. M. Law, and M. J. W. Rodwell, Appl. Phys. Express **4**, 091102 (2011).
[4] V. Chobpattana, J. Son, J. J. M. Law, R. Engel-Herbert, C. Y. Huang, and S. Stemmer, Appl. Phys. Lett. **102**, 022907 (2013).
[5] V. Chobpattana, T. E. Mates, W. J. Mitchell, J. Y. Zhang, and S. Stemmer, J. Appl. Phys. **114**, 154108 (2013).
[6] S. Lee, C.-Y. Huang, D. Cohen-Elias, J. J. M. Law, V. Chobpattanna, S. Krämer, B. J. Thibeault, W. Mitchell, S. Stemmer, A. C. Gossard *et al.*, Appl. Phys. Lett. **103**, 233503 (2013).
[7] X. Y. Zhao and D. Vanderbilt, Phys. Rev. B **65**, 233106 (2002).
[8] X. Y. Zhao and D. Vanderbilt, Phys. Rev. B **65**, 075105 (2002).
[9] S. Koveshnikov, N. Goel, P. Majhi, H. Wen, M. B. Santos, S. Oktyabrsky, V. Tokranov, R. Kambhampati, R. Moore, F. Zhu *et al.*, Appl. Phys. Lett. **92**, 222904 (2008).
[10] L. Lamagna, A. Molle, C. Wiemer, S. Spiga, C. Grazianetti, G. Congedo, and M. Fanciulli, J. Electrochem. Soc. **159**, H220 (2012).
[11] R. Engel-Herbert, Y. Hwang, J. Cagnon, and S. Stemmer, Appl. Phys. Lett. **95**, 062908 (2009).
[12] J. Huang, N. Goel, H. Zhao, C. Y. Kang, K. S. Min, G. Bersuker, S. Oktyabrsky, C. K. Gaspe, M. B. Santos, P. Majhi *et al.*, 2009 Tech. Dig. - Int. Electron Devices Meet. **2009**, 308.
[13] M. Passlack, M. Hong, E. F. Schubert, G. J. Zydzik, J. P. Mannaerts, W. S. Hobson, and T. D. Harris, J. Appl. Phys. **81**, 7647 (1997).
[14] R. Engel-Herbert, Y. Hwang, and S. Stemmer, J. Appl. Phys. **108**, 124101 (2010).
[15] M. El Kazzi, L. Czornomaz, C. Rossel, C. Gerl, D. Caimi, H. Siegwart, J. Fompeyrine, and C. Marchiori, Appl. Phys. Lett. **100**, 063505 (2012).
[16] R. Suzuki, N. Taoka, M. Yokoyama, S. Lee, S. H. Kim, T. Hoshii, T. Yasuda, W. Jevasuwan, T. Maeda, O. Ichikawa *et al.*, Appl. Phys. Lett. **100**, 132906 (2012).
[17] K. Martens, C. O. Chui, G. Brammertz, B. De Jaeger, D. Kuzum, M. Meuris, M. M. Heyns, T. Krishnamohan, K. Saraswat, H. E. Maes *et al.*, IEEE Trans. Electron Devices **55**, 547 (2008).
[18] I. Krylov, L. Kornblum, A. Gavrilov, D. Ritter, and M. Eizenberg, Appl. Phys. Lett. **100**, 173508 (2012).
[19] H. C. Lin, G. Brammertz, K. Martens, G. de Valicourt, L. Negre, W. E. Wang, W. Tsai, M. Meuris, and M. Heyns, Appl. Phys. Lett. **94**, 153508 (2009).
[20] E. H. Nicollian and J. R. Brews, *MOS (Metal Oxide Semiconductor) Physics and Technology* (Wiley, New York, 1982).
[21] X. Y. Zhao, D. Ceresoli, and D. Vanderbilt, Phys. Rev. B **71**, 085107 (2005).
[22] R. Engel-Herbert, Y. Hwang, and S. Stemmer, Appl. Phys. Lett. **97**, 062905 (2010).
[23] H. P. Chen, Y. Yuan, B. Yu, C. S. Chang, C. Wann, and Y. Taur, Semicond. Sci. Technol. **28**, 085008 (2013).
[24] N. Taoka, M. Yokoyama, S. H. Kim, R. Suzuki, S. Lee, R. Iida, T. Hoshii, W. Jevasuwan, T. Maeda, T. Yasuda *et al.*, IEEE Trans. Device Mater. Reliab. **13**, 456 (2013).

[25] M. Procop, J. Electron Spectrosc. Relat. Phenom. **59**, R1 (1992).
[26] T. Gougousi, J. C. Hackley, J. D. Demaree, and J. W. Lacis, J. Electrochem. Soc. **157**, H551 (2010).
[27] B. V. Crist, *Handbook of Monochromatic XPS Spectra* (Wiley, New York, 2000).
[28] R. J. Hussey, G. I. Sproule, J. P. McCaffrey, and M. J. Graham, Oxid. Met. **57**, 427 (2002).
[29] L. Lin and J. Robertson, J. Vac. Sci. Technol. B **30**, 04E101 (2012).
[30] H. P. Komsa and A. Pasquarello, Physica B **407**, 2833 (2012).
[31] L. Lin and J. Robertson, Appl. Phys. Lett. **98**, 082903 (2011).